JOURNAL OF CATALYSIS 123, 147–156 (1990)

Redox Properties of Chromic Acid Supported on Silica

W. HILL AND G. ÖHLMANN

Zentralinstitut für Physikalische Chemie, Akademie der Wissenschaften der DDR, DDR-1199 Berlin-Adlershof, German Democratic Republic

Received April 28, 1989; revised November 10, 1989

Redox properties of chromium/silica catalysts prepared by impregnation of silica with an aqueous solution of CrO_3 are studied for chromium contents between 10^{-3} and 1% by weight. Temperature-programmed experiments and spectroscopic data are used to characterize the kinetics and final states of reduction by hydrogen and ethanol as well as the oxidation of reduced samples by molecular oxygen. The oxidation of hydroxylated Cr^{3+} species to Cr^{6+} exhibits an activation energy of 113 kJ/mol. © 1990 Academic Press, Inc.

INTRODUCTION

The partial oxidation of alcohols by silica-supported chromic acid (*1, 2*) and the elucidation of the oxidation state of chromium active in ethylene polymerisation with these catalysts (*3–8*) raise the question of the redox properties of supported chromic acid. Even in freshly prepared Cr/SiO_2 catalysts not all the chromium is present as Cr^{6+} ions. In particular at low chromium content partial reduction is evident, as will be shown later. During calcination at temperatures above 873 K a nearly complete oxidation to Cr^{6+} is possible, if conversion to α-Cr_2O_3 can be avoided (*7, 9*).

The reduction of Cr^{6+}/SiO_2 by CO leads mainly to Cr^{2+} (*5–8, 10–14*), in which average oxidation numbers lie between 2.5 (*7*) and 2.1 (*10*). A dependence of the degree of reduction on chromium content has not been observable (*15*), but an intermediate formation of Cr^{5+} and Cr^{3+} could be detected (*16*). Thorough investigations of the reduction of Cr^{6+}/SiO_2 by hydrogen have shown that this reduction leads mainly to Cr^{3+}, but with efficient water removal a large amount of Cr^{2+} is formed (*1, 6, 7, 17*). This may be explained by the formation of three-dimensional, no longer reducible Cr^{3+} aggregates in the presence of water (*6*) or by the oxidation of Cr^{2+} to Cr^{3+} by water. Two peaks at 615 and 745 K in temperature-programmed reduction spectra have been assigned by one of us (*1*) to hexavalent chromium in different aggregation stages. With ethylene there occurs a nearly quantitative reduction of Cr^{6+} on silica to Cr^{2+} (*18*).

On irradiation near the red limit of the charge-transfer region, photoreduction of Cr^{6+}/SiO_2 in hydrogen occurs, leading to Cr^{5+}, and a further reduction results with higher quantum energies. During photoreduction with CO, Cr^{2+} and possibly Cr^{4+} are formed (*14, 19*).

Coordinatively unsaturated Cr^{2+} on SiO_2 is oxidized by molecular oxygen to Cr^{6+} without notable activation energy. This reaction proceeds already at room temperature with the emission of red luminescence. Between 25 and 70% of the chromium on CO-reduced samples are oxidized in this way (*10, 11, 18, 20, 21*). The amount of chromium reacting with oxygen at room temperature is lowered distinctly with thermal treatment of reduced samples under vacuum (*10, 11*). An activated oxidation of the residual chromium between ca. 773 and 873 K is considered to be due to the existence of higher coordinated Cr^{2+} (*10, 11, 20*).

Water with partial pressure above 10^4 Pa and also silanols cause a slow oxidation of Cr^{2+} to Cr^{3+} at elevated temperatures (*4, 7*).

Cr^{5+} in solution is not stable because it

0021-9517/90 $3.00

usually quickly disproportionates to Cr^{3+} and Cr^{6+} (*22*). Cr^{5+} fixed on the silica surface, however, can be very stable and it is detectable even after hydrogen or oxygen treatment at temperatures above 770 K (*7, 19*). Cr^{5+} on silica appears as a relatively stable intermediate in the reduction of Cr^{6+} by CO as well as in the oxidation of Cr^{3+}-containing samples (*1, 16*).

The redox properties of Cr^{3+} ions depend essentially on their coordination (*20*). Dispersed Cr^{3+} on silica can be oxidized to Cr^{5+} by oxygen at 673 K within 1 h (*16*). Crystalline Cr_2O_3 is widely stable even to reduction, while dispersed Cr^{3+} is reducible with CO (*16*). Adsorption of oxygen at coordinatively unsaturated Cr^{3+} leads to the formation of O^- radicals (*23*).

Little is known about the properties of Cr^{4+} on SiO_2 because it cannot be reliably detected. Its formation has been proposed only in photoinduced reactions (*4, 14*).

This paper reports a temperature-programmed and spectroscopic study of the reduction of Cr^{6+}/SiO_2 with hydrogen and ethanol, respectively, and of the reaction of reduced catalysts with oxygen.

EXPERIMENTAL

Catalysts

Catalysts containing 1.0×10^{-3}, 1.0×10^{-2}, 1.0×10^{-1}, or 1.0% (by weight) of chromium are prepared by dry impregnation of previously granulated Degussa aerosil Ae300 or Ox50 with 1 cm^3/g of a titrated solution of CrO_3 (pa) in distilled water as described earlier (*2*). The aerosils have specific surface areas of around 300 m^2/g (Ae300) and 50 m^2/g (Ox50). The impregnated silica is dried for 2 h at 423 K in a stream of air before storage.

Materials

Helium is purified by passage through a column filled with copper catalyst (Leuna-Kontakt 4492). Traces of water are removed from all gases in a molecular sieve column (Wolfen-Zeosorb 5A). Gases are mixed in a previously evacuated gas cylinder. The gas mixture for TPR contains 5.0 vol% hydrogen in helium and that for TPO had 1.3 vol% oxygen in the same carrier gas. Ethanol (absolute, purissimum, from VEB Laborchemie Apolda) has been thoroughly degassed before each experiment.

Temperature-Programmed Investigations

Apparatus

Temperature-programmed measurements are performed at normal pressure with a gas flow system consisting of a gas purifier, flow controllers, a thermostated evaporator for ethanol, a gas-mixing device, the reactor, and a flow meter. A part of the gas is introduced into a calibrated quadrupole mass spectrometer coupled with a peak selector, which allows a fast analysis of masses of interest between 2 and 80 a.m.u. The tubes containing ethanol vapour or product gases and the vacuum inlet are made of refined steel, and they must be heated to prevent condensation. Tubes of quartz glass with volumes corresponding to the catalyst volume serve as reactors. The catalyst is placed on a frit and a thermocouple can be situated inside the catalyst bed via a quartz insert. The heating system consists of a temperature programmer for linear heating and a radiant heat furnace. Furnace dimensions are about 10 times those of the reactor, so temperature gradients in the catalyst bed can be avoided.

(*a*) *Temperature-programmed reduction (TPR) and temperature-programmed oxidation (TPO).* Temperature-programmed reduction/oxidation is carried out in 5.0 vol% H_2/He or 1.3 vol% O_2/He, respectively, with a flow rate of 0.2 dm^3/h. Samples with a weight of 0.2 g (1 wt% Cr) or 2.0 g (0.1 wt% Cr) are heated with a rate of 10 K/min from room temperature (293 K) to 973 K. TPO, TPR, and oxidation at room temperature are performed cyclically in some cases. In these cycles samples are

flushed with helium at 973 K after TPR and TPO and cooled under helium to avoid adsorption of hydrogen or oxygen during cooling. The oxygen uptake of the reduced samples at room temperature is determined from the breakthrough curve of oxygen, corrected for the response of the reactor system.

(*b*) *Temperature-programmed surface reactions (TPSR) with ethanol.* The TPSR of catalysts with ethanol are performed in each case with 1.6 g of catalyst, which is pretreated *in situ* with dry air (1.8 dm^3/h) by drying at 423 K for 0.5 h, followed by oxidation, then temperature programmed with a heating rate of 10 K/min to 873 K, and finally maintained for 0.5 h at a constant temperature of 873 K. After this treatment the samples are held under flowing helium at 873 K until no more oxygen can be detected in the exit gas by mass spectrometry. After that 8 mol ethanol per mole Cr is admitted at room temperature by passing a flow of ethanol containing helium (with a flow rate of 2.3 dm^3/h and a content of 5.2 vol%) over the catalyst. After completion of the ethanol adsorption the temperature is increased with a rate of 4.0 K/min, while 0.30 dm^3/h (0.10% Cr/Ae300) or 1.0 dm^3/h (1.0% Cr/Ae300) pure helium flows over the catalyst.

For TPSR the pure silica is handled in the same way as is the catalyst containing 1.0% Cr. The reproducibility of all results of temperature-programmed investigations has been proved by repeating the experiments at least once.

UV–Visible Diffuse Reflection

UV–visible diffuse reflection spectra are measured with a Beckman DK2A spectrometer using silica Ae300 (dehydroxylated at 1073 K) as reference. Catalysts for UV–visible diffuse reflection spectroscopy are broken up in a mortar and then dried and oxidized in a muffle furnace (30 min at 423 K; heating slowly for 1 h to 873 K and then 30 min at this temperature). The hot samples are transferred into optical cells, which are immediately evacuated to 0.01 Pa.

For adsorption the catalysts were held under ethanol vapour for 5 min at room temperature. Afterward, the samples are degassed at room temperature, carefully heated under (dynamic) vacuum to the desired temperature (373 K, 473 K, or 623 K), kept isothermal for 10 min, cooled down, measured, and heated to the next higher temperature.

Calculation of Activation Energy

The activation energy of oxidation is determined by fitting a theoretical curve to 40 points of the measured TPO peak. The mathematical model is analogous to that developed earlier for TPR (*17*). Assumptions of reaction order for oxygen equal to one in the initial oxidation step and of fast subsequent steps are justified by good coincidence of measured and calculated oxidation profiles.

RESULTS

Reduction with Hydrogen

The reduction of untreated samples and that of samples oxidized previously at 973 K occurs completely, resulting in a peak with a maximum temperature of 750 ± 10 K in most cases (Fig. 1). An additional small peak around 875 K was only observable for the nonpretreated 0.1% Cr/Ae300 catalyst (Fig. 1b). Table 1 summarizes the hydrogen consumption during TPR with and without preceding redox treatment. The hydrogen uptake during TPR for 1.0% Cr/Ae300 re-

TABLE 1

Hydrogen Consumption during TPR (mol/mol_{Cr})

Pretreatment	Catalyst		
	0.1% Cr/Ae300	1.0% Cr/Ae300	1.0% Cr/Ox50
—	0.26	1.46	1.50
TPO	1.60	1.47	0.49

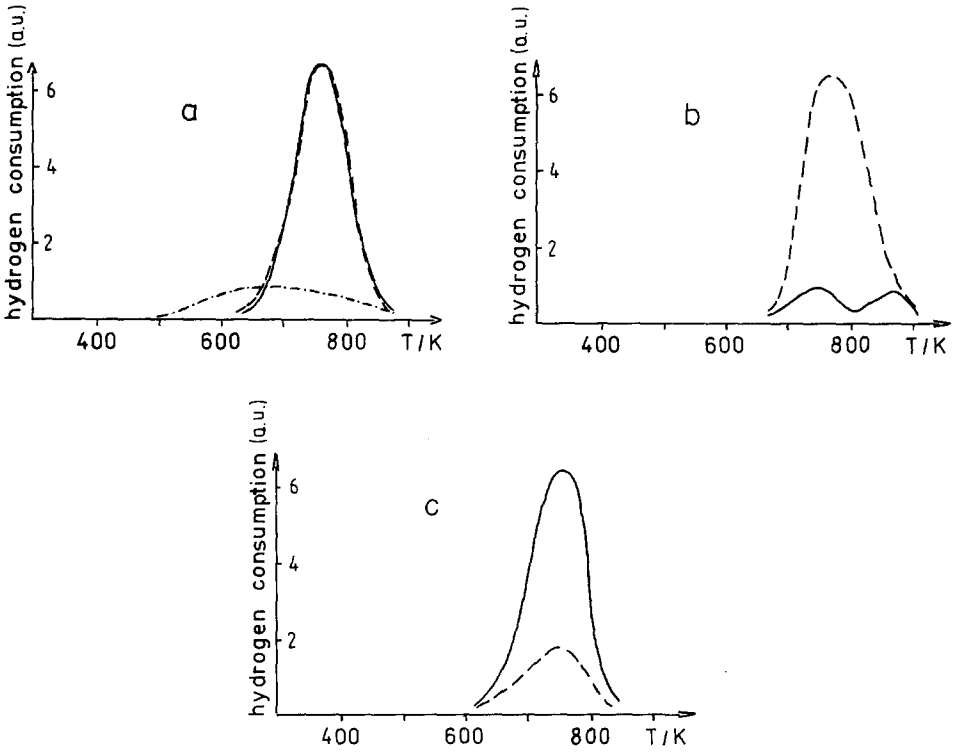

FIG. 1. TPR spectra of 1% Cr/Ae300 (a), 0.1% Cr/Ae300 (b), and 1% Cr/Ox50 (c) without pretreatment (——), after TPO (– – –), and after TPR followed by oxidation at 293 K (– · – · –).

mains constant within the margin of error of our measurements over several cycles of consecutive TPR and TPO. The same applies to 0.10% Cr/Ae300 after the first TPO. For 1.0% Cr/Ox50 a diminution of the hydrogen uptake by two-thirds takes place after redox treatment as well as after simple heating under helium [heating under helium was performed as in the investigations on thermal decomposition of such catalysts (*24*)].

A more detailed investigation of the 1.0% Cr/Ae300 catalyst shows that a comparatively broad reduction peak (300 K halfwidth) appears around 680 K during TPR conducted after an initial TPR which had been followed by oxygen admission at room temperature (see Fig. 1a, dot-dashed curve). The peak area corresponds to a hydrogen consumption of (0.37 ± 0.03) mol H_2/mol Cr. Hydrogen uptake for this catalyst at room temperature is not observable within the detection limit (about 0.02 mol H_2/mol Cr), neither after TPO nor after TPR followed by oxidation at room temperature.

During TPR experiments a small, and initially nearly constant, hydrogen consumption remains at temperatures above the reduction peaks. This consumption is likely to be due to the known reoxidation of reduced species by hydroxyls (*7*), and it is disregarded in the interpretation of the TPR curves.

Reduction with Ethanol

(*a*) *TPSR.* Both the chromium catalysts (containing 0.10 and 1.0% Cr on Ae300) and the pure silica Ae300 adsorb completely the ethanol admitted at room temperature without detectable release of products at this temperature. The ethanol adsorption ca-

pacity of pure silica is considerably higher than the amount admitted before TPSR (even 10 mmol ethanol/g silica is adsorbed completely).

During temperature-programmed heating silica desorbs ethanol in a peak with a maximum temperature of 410 K. Silica does not release other products below 670 K. The catalysts additionally desorb acetaldehyde within a narrow peak with a half-value width of around 20 K immediately at the beginning of the ethanol peak. The peak maximum temperature of acetaldehyde corresponds to 370 K. The quantity of acetaldehyde is 1.5 ± 0.2 mol/mol$_{Cr}$ (derived from five measurements). The considerable uncertainty in the determination of this value results from the overlapping with the desorption of larger amounts of ethanol.

Further products are released above 470 K (butadiene with peak-maximum temperature 490 K, butene 560 K, methane and carbon dioxide 710 K) (*25*). These products cannot be unambiguously related to the redox properties of chromium on silica and therefore they are not considered in this paper.

(*b*) *UV–visible diffuse reflection.* Qualitatively very similar spectra are obtained for catalysts containing 0.0010, 0.010, 0.10, or 1.0% Cr/Ae300. Figure 2 shows the spectra of the 0.10% catalyst. After pretreatment only the intense bands near 245, 345, and 455 nm characteristic of Cr^{6+} appear.

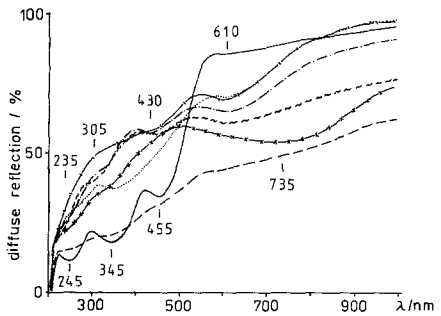

FIG. 2. UV–visible diffuse reflection of 0.1% Cr/Ae300 after pretreatment (——); after adsorption of ethanol at 293 K (· · ·); degassed at 293 K (–/–/–), 373 K (–·–·–), 473 K (~~~), and 623 K (x–x–x); after exposure to air at 293 K (– – –).

After adsorption of ethanol at room temperature the bands at 245 and 455 nm disappear and a medium strong or weak band at 610 nm emerges. At lower chromium content a weak shoulder appears around 430 nm. The extinction of the 345-nm band is distinctly lowered by adsorption of ethanol. During admission of ethanol a decoloration proceeds within seconds for samples with low Cr content and a change of colour from yellow to grey-green occurs for the other samples.

After evacuation at room temperature the ~610-nm band shifts slightly to ~590 nm, a distinct shoulder emerges at ~430 nm, and the ~345-nm band disappears nearly completely. Degassing at 373 K brings new bands near 305, 430, and 610 nm and a shoulder at ~235 nm. The latter is better observable for lower chromium content and is probably overlapped by the strong adsorption in this region for higher Cr content. After evacuation at 473 K the shoulder at 235 nm disappears, the band near 305 nm becomes weaker, and the 610-nm band shifts to 620 nm. Heating to 623 K causes a broadened absorption in the charge-transfer region as well as a strong broadening and increase in the extinction of the band above 600 nm with a wavelength shift to 630 nm (1.0% Cr), 735 nm (0.10% Cr), or 750 nm (below 0.10% Cr), respectively.

Admission of air at room temperature removes the latter band leaving a weak shoulder at 625 nm and leads to an absorption in the whole visible region with a higher extinction for higher energy light quanta and with shoulders at the positions of Cr^{6+} bands.

ESR investigations of 0.10% Cr/Ae300 and 1.0% Cr/Ae300 using the same kind of procedure as for UV–visible diffuse reflection shows no $Cr^{3+}(\delta)$-signal, neither after ethanol adsorption nor after degassing at the given temperatures.

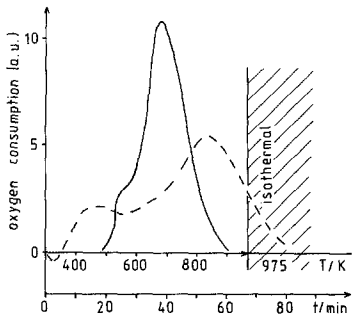

FIG. 3. TPO of 0.1% Cr/Ae300 without pretreatment (——) and after TPO followed by TPR (– – –).

Oxidation

During TPO fresh 0.10% Cr/Ae300 samples take up between 0.4 and 1.0 mol O_2/mol Cr in a peak at 680 K (Fig. 3). After TPR and oxygen admission at room temperature 0.10% Cr/Ae300 desorbs some oxygen (7 mmol O_2/mol Cr) around 330 K during TPO.

The catalysts take up oxygen at room temperature after TPR (Table 2). During TPO all chromium catalysts exhibit a peak at 830 K comprising the main part of oxygen uptake (Figs. 3 and 4). The TPO spectrum of 0.10% Cr/Ae300 shows additionally a peak at 450 K representing around 20% of the total oxygen consumption. The width and shape of this curve point to the existence of additional but not resolved peaks.

Table 2 contains the values of oxygen consumption during oxidation and hydrogen uptake during TPR before and after TPO for different catalysts.

In TPO experiments with hydrogen-reduced samples a water release is observed during and immediately after oxidation (Fig. 4). Such a water release does not appear during heating of reduced samples under helium.

UV–visible spectra of hydrogen-reduced 1.0% Cr/Ae300 after oxygen admission at room temperature and after TPO show in both cases only the three bands at 245, 345, and 455 nm which are typical for Cr^{6+}, but with a higher extinction after TPO. TPR and TPO of pure silica Ae300 under the same conditions as those for the 0.10% Cr/Ae300 do not show any reduction or oxidation peak within the detection limit. Numerical fitting of the TPO curve of 1.0% Cr/Ae300 gives an activation energy of the 830-K peak of E_a = 113 kJ/mol.

After TPSR with ethanol to a temperature of 430 K, where the release of acetaldehyde is completed, the 0.1% Cr/Ae300 does not take up oxygen at room temperature. The same experiment with a final temperature of TPSR of 573 K, that is after release of butadiene and butene, leads to an oxygen uptake of 0.17 mol/mol_{Cr}.

TABLE 2

Oxygen/Hydrogen Consumption during Oxidation/Reduction in mol/mol_{Cr}

Treatment	Catalyst		
	0.1% Cr/Ae300[a]	1.0% Cr/Ae300	1.0% Cr/Ox50
1. TPR	1.54	1.54	1.50
2. O_2 at 295 K	0.14	0.09	0.05
3. TPO	0.63	0.69	0.34
4. TPR	1.60	1.47	0.49

[a] Sample was previously oxidized by TPO.

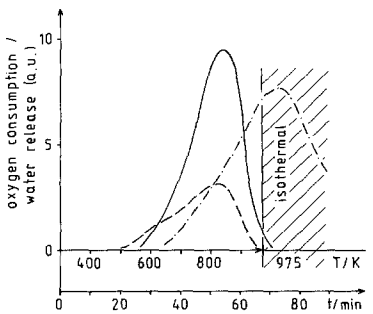

FIG. 4. TPO of 1.0% Cr/Ae300 [oxygen consumption (——), water release (– · – · –)] and 1.0% Cr/Ox50 [oxygen consumption (– – –)] after TPO followed by TPR.

DISCUSSION

Reduction with Hydrogen

The absence of a reduction peak around 615 K for the 1.0% Cr/Ox50 sample seems to contradict former results in which such a peak for a sample of the same composition had a larger area than that of the peak at 705 K (*17*). However, the impregnation of the formerly investigated catalysts was performed with larger amounts of solution, and consequently the evaporation of the residual liquid resulted in inhomogenities of the active phase. Therefore, the peak at 615 K must be due to aggregates formed under particular preparation conditions. A comparison with thermal decomposition of the catalysts of the same kind as those in this paper (*24*) shows, however, that aggregates which are thermally more stable than pure CrO_3, because of interaction with the support, are not reduced in this low temperature peak.

Investigations of thermal decomposition and of photoluminescence of chromium catalysts (*24, 26*) have revealed the existence of several monomeric, aggregated, and even thermally unstable chromium species on catalysts now subjected to TPR. All these species are evidently reduced in the peak at 750 K. Therefore, it would be quite natural to relate the 615-K peak to bulk-like aggregates of CrO_3, which decompose thermally at temperatures near the low temperature peak of TPR (*24*).

The amount of chromium on 1.0% Cr/Ox50, which can be reversibly reduced and oxidized, agrees quite well with the amount of thermally stable chromium determined by thermal decomposition (*24*). The TPR of thermally treated samples shows on the one hand that thermally stable species are completely reoxidized by TPO after TPR. On the other hand, thermally unstable species are not reoxidisable after reduction or thermal decomposition.

The small hydrogen consumption of nonpretreated samples with lower chromium content is probably a consequence of reduction caused by impurities from the air during storage (see also the later discussion of oxidation).

The broad TPR peak of 1.0% Cr/Ae300 after TPR and oxygen admission at room temperature is due to the overlap of at least two peaks. Since we know from the UV–visible spectrum that there is Cr^{6+} on the sample, one of these peaks can be attributed to the reduction of Cr^{6+} around 750 K. In this case, there must be a second, more easily reducible, species on the sample, which causes a TPR peak around 610 K. Attempts to identify this species by ESR and UV–visible spectroscopy have failed because there has been no signal that has changed during reduction at these temperatures.

Reduction with Ethanol

The results do not give any evidence for a dependence of reduction by ethanol at room temperature on chromium content or structure of chromium species. The Cr^{6+}/silica catalysts are readily reduced to Cr^{3+} by ethanol at low temperatures with formation of acetaldehyde. The formation of Cr^{3+} is supported by the amount of acetaldehyde in TPSR and by the spectroscopic measurements. Visual observations show that the reaction between Cr^{6+} and ethanol occurs fast even at room temperature. After ethanol adsorption a band near 600 nm appears. A second band, which can also be caused by octahedrally coordinated Cr^{3+}, emerges at 430 nm after evacuation. The 430- and 600-nm bands have wavelengths characteristic for $^4A_{2g} \rightarrow {}^4T_{1g}$ and $^4A_{2g} \rightarrow {}^4T_{2g}$ transitions of octahedral Cr^{3+} complexes with oxygen ligands and the reduced Racah parameter of these bands ($B \sim 650$ cm^{-1}) agrees with known values of such complexes (*27*). The reason for the development of the 430-nm band only after evacuation and the existence of a 345-nm band in the presence of ethanol vapour is not quite clear, but it should be related to the interaction of reduced chromium with adsorbed

ethanol or the reaction product acetaldehyde.

The release of acetaldehyde in the TPSR takes place in a peak around 370 K, whereas the UV–visible diffuse reflection reveals the reduction of chromium even at room temperature. Such a difference could originate from an activated desorption of acetaldehyde. However, the position of the very small acetaldehyde desorption peak immediately at the beginning of ethanol desorption from silica and the large ethanol adsorption capacity of silica lead to the conclusion that during TPSR at first the admitted ethanol has been nearly completely adsorbed on the silica and affects the chromium after desorption from silica only, whereas the samples for UV–visible spectroscopy are penetrated with ethanol already after ethanol vapour treatment.

A reduction of isolated surface monochromate to Cr^{3+} by ethanol at low temperature is unlikely for chemical reasons. Indeed, this reduction should not occur following the absence of a ESR $Cr^{3+}(\delta)$-signal in the reduced samples. On the other hand, Cr^{6+} bands at 245 and 455 nm in the UV–visible spectra disappear completely at room temperature even at the lowest chromium content. There is no spectroscopic evidence for different oxidation states of chromium in different aggregates at this temperature. The reduction of monochromate possibly leads to a species which is difficult to detect by the applied methods, such as Cr^{4+}. However, the absence of the poorly detectable δ-signal is no reliable proof for the complete absence of monomeric Cr^{3+}.

The intensity decrease of the Cr^{3+} bands and the formation of a new band above 750 nm, which is only discernable as a shift and extinction change of the 600-nm band because of its width, point to a further reduction of the catalysts above 473 K. The position of the new band and the instantaneous oxidation of the reduced samples at room temperature refer to Cr^{2+} as final state of reduction. The reduction to Cr^{2+} occurs slowly and is incomplete even after treatment at 623 K. The more pronounced shift of the band at lower chromium content points to a higher amount of Cr^{2+}, which might be due to an easier reduction of the intermediate originating from surface monochromate compared with the more stable Cr^{3+} aggregates.

The partial reduction of Cr^{3+} to Cr^{2+} at higher temperatures is confirmed by the oxygen uptake of the sample previously subjected to TPSR with higher final temperature.

Oxidation

The TPO peak of nonpretreated samples containing 0.10% Cr lies in a temperature region where, according to other temperature-programmed investigations (*25*), organics are oxidized to CO_2 by these catalysts. Moreover, the large oxygen uptake without preceding reduction, the distinctly different peak areas for different samples of the same chromium content, and the results of TPR point to an adsorption of organics during storage. Thus, the interpretation is reasonable that the 680-K TPO peak originates from the oxidation of organics.

Oxygen uptake at room temperature and the TPO peak areas of prereduced samples do not obey a stoichiometric ratio. Thus the peaks and the oxidation at room temperature must be related to different chromium species and not to a stepwise oxidation of one species.

The hydrogen consumption during TPR shows the expected predominant reduction to Cr^{3+}. Furthermore, the main portion of chromium is present as Cr^{6+} after TPO, at least on Ae300. Therefore, it is obvious that the dominating TPO peak at 830 K must be ascribed to the oxidation of Cr^{3+} to Cr^{6+}. Not all Cr^{3+} species are oxidized in this peak as inferred from the Ox50 experiment. The bulk-like Cr_2O_3 on this support does not take up oxygen up to 973 K.

Water release during and after oxidation proves the presence of hydroxyls in the reduced species. A comparison with ESR

results shows the intermediate formation of Cr^{5+} during oxidation of Cr^{3+} at these temperatures (*1*).

The oxidation at room temperature, which leads to Cr^{6+}, can be related to divalent chromium, as discussed in earlier papers (*10, 11, 28*). The TPO peak at 450 K appearing at lower chromium content could be due to monomeric Cr^{3+}, but could also arise from an activated oxidation of higher coordinated Cr^{2+} (*11*).

CONCLUSIONS

The earlier observed TPR peak at 615 K (*1, 17*) should be related to bulk-like CrO_3 on silica. Other monomeric and aggregated Cr^{6+} species, which are stabilized by dispersion and fixation on the support, are reduced within a TPR peak at 750 K. The reduction of thermally stable species with hydrogen is completely reversible by TPO. The oxidation of hydrogen-reduced catalysts at room temperature leads to Cr^{6+} and a species which is more easily reducible than Cr^{6+}.

Ethanol readily reduces the whole of the Cr^{6+} on silica with formation of acetaldehyde. This reduction leads to Cr^{3+}, at least for aggregated chromium species. During degassing of ethanol-reduced catalysts a further reduction to Cr^{2+} takes place at higher temperatures.

Thermally unstable chromium species cannot be oxidized after reduction or thermal decomposition up to 973 K. Cr^{3+} species which are formed by reduction of thermally stable, aggregated Cr^{6+} contain hydroxyls and are oxidized by molecular oxygen to Cr^{6+} with an activation energy of 113 kJ/mol. Additionally, a more easily oxidizable species is detected after reduction of catalysts with lower chromium content.

The ease of acetaldehyde formation from ethanol with simultaneous reduction of Cr^{6+} to Cr^{3+} and the coincidence of the activation energies for reoxidation of Cr^{3+} and catalytic oxidation of ethanol with chromium catalysts of higher chromium contents (*1*) show that catalysis proceeds via the redox mechanism Cr^{6+}/Cr^{3+} with reoxidation of the catalyst as the limiting step. At lower chromium contents the catalysis is dominated by other mechanisms (*29*), which might include the more easily oxidizable species detected in this investigation.

ACKNOWLEDGMENTS

The authors thank Drs. M. Richter, W. Hanke, and R. Fricke for discussion and performing UV–visible and ESR investigations.

REFERENCES

1. Parlitz, B., Hanke, W., Fricke, R., Richter, M., Roost, U., and Öhlmann, G., *J. Catal.* **94,** 24 (1985).
2. Richter, M., and Öhlmann, G., *React. Kinet. Catal. Lett.* **29,** 211 (1985).
3. Zecchina, A., Garrone, E., Morterra G., and Borello, E., *J. Phys. Chem.* **79,** 966 (1965).
4. Pr'shevalskaja, L. K., Shvets, V. A., and Kazansky, V. B., *Kinet. Katal.* **11,** 1310 (1970).
5. Krauss, H. L., *in* "Proceedings, 5th International Congress on Catalysis, Palm Beach, 1972" (J. W. Hightower, Ed.), Vol. 1, p. 207. North-Holland, Amsterdam, 1973.
6. Hogan, J. P., *J. Polym. Sci. A-1* **8,** 2637 (1970).
7. Groeneveld, C., Wittgen, P. P. M. M., van Kersbergen, A. M., Mestrom, P. L. M., Nuijten, C. E., and Schuit, G. C. A., *J. Catal.* **59,** 153 (1979).
8. Myers, D. L., and Lunsford, J. H., *J. Catal.* **92,** 260 (1985).
9. McDaniel, M. P., *J. Catal.* **76,** 17 (1982).
10. Ghiotti, G., Garrone, E., Della Gatta, G., Fubini, B., and Giamello, E., *J. Catal.* **80,** 249 (1983).
11. Fubini, B., Ghiotti, G., Stradella, L., Garrone E., and Morterra, C., *J. Catal.* **66,** 200 (1980).
12. Merryfield, R., McDaniel, M. P., and Parks, G., *J. Catal.* **77,** 348 (1982).
13. Best, S. A., Squires, R. G., and Walton, R. A., *J. Catal.* **47,** 292 (1977).
14. Kazansky, V. B., Pershin, A. N., and Shelimov, B. N., *in* "Proceedings, 7th International Congress on Catalysis, Tokyo, 1980" (T. Seiyama and K. Tanabe, Eds.), p. 1210. Elsevier, Amsterdam, 1981.
15. Krauss, H. L., and Westphal, U., *Z. Anorg. Allg. Chem.* **430,** 218 (1977).
16. Beck, D. D., and Lunsford, J. H., *J. Catal.* **68,** 121 (1981).
17. Ehrhard, K., Richter, M., Roost, U., and Öhlmann, G., *Appl. Catal.* **17,** 23 (1985).
18. Baker, L. M., and Carrick, W. L., *J. Org. Chem.* **33,** 616 (1968).
19. Pershin, A. N., Shelimov, B. N., and Kazansky, V. B., *Kinet. Katal.* **22,** 1526 (1981).

20. McDaniel, M. P., and Welch, M. B., *J. Catal.* **82,** 110 (1983).
21. Morys, P., Görges, U., and Krauss, H. L., *Z. Naturforsch. B. Anorg. Chem. Org. Chem.* **39,** 458 (1984).
22. Krumpolc, M., and Rocek, J., *J. Amer. Chem. Soc.* **98,** 872 (1976).
23. Shvets, V. A., Lipatkina, N. I., Kazansky, V. B., and Chuvylkin, N. D., *in* "Magnetic Resonance in Colloid and Interface Science" (J. P. Fraissard and H. A. Resing, Eds.), NATO ASI Ser. C, p. 521. Reidel, Dordrecht, 1980.
24. Hill, W., and Öhlmann, G., *React. Kinet. Catal. Lett.* **38,** 289 (1989).
25. Hill, W., and Öhlmann, G., unpublished.
26. Hill, W., Shelimov, B. N., Kibardina, I. R., and Kazansky, V. B., *React. Kinet. Catal. Lett.* **31,** 315 (1986).
27. Stojaković, D., and Vasović, D., *Monatsh. Chem.* **116,** 581 (1985).
28. Krauss, H. L., and Stach, H., *Z. Anorg. Allg. Chem.* **366,** 34 (1966).
29. Hill, W., Miessner, H., and Öhlmann, G., *J. Chem. Soc. Faraday Trans. 1* **85,** 691 (1989).